TRYPTOPHAN SIDECHAIN DYNAMICS IN HYDROPHOBIC OLIGOPEPTIDES DETERMINED BY USE OF ^{13}C NUCLEAR MAGNETIC RESONANCE SPECTROSCOPY

ARTHUR J. WEAVER,* MARVIN D. KEMPLE,‡ and FRANKLYN G. PRENDERGAST*
*Department of Biochemistry and Molecular Biology, Mayo Foundation, Rochester, Minnesota 55905; and ‡Department of Physics, Indiana University–Purdue University at Indianapolis (IUPUI), Indianapolis, Indiana 46223

ABSTRACT Two oligopeptides, *t*-boc-LAWAL-OMe and *t*-boc-LALALW-OMe, were synthesized for the purpose of examining the sidechain dynamics of the tryptophan residue in hydrophobic environments by ^{13}C nuclear magnetic resonance and fluorescence spectroscopy. In both peptides, the tryptophan sidechain was >95% enriched with ^{13}C at the $C\delta_1$ position. Spin-lattice relaxation time (T_1) and steady-state nuclear Overhauser effect (NOE) data were obtained at 50.3 and 75.4 MHz for both peptides in CD_3OD, and at 75.4 MHz for *t*-boc-LALALW-OMe in lysolecithin-D_2O micelles. We have adapted the model-free approach of G. Lipari and A. Szabo (1982, *J. Am. Chem. Soc.* 104:4546) to interpret the ^{13}C-NMR data. Computer-generated curves based on experimental data obtained at a single frequency demonstrate relationships between an effective correlation time for tryptophan sidechain motion (τ_e), a generalized order parameter ($\mathcal{S}$) describing the extent of motional restriction, and an overall correlation time for the peptide (τ_m). Assuming predominantly dipolar relaxation, least-squares fits of the dual frequency relaxation data provide values for these parameters for both peptides. The contribution of chemical shift anisotropy (CSA), however, is also explicitly assessed in the data analysis, and is shown to perturb the predicted $\mathcal{S}$, τ_e, and τ_m values and to decrease χ^2 values observed in nonlinear least-squares analysis of the data. Because of uncertainty in the contribution of CSA to the relaxation of the indole ring $^{13}C\delta_1$ atom, nonlinear least-squares analysis of the relaxation data were performed with and without inclusion of a CSA term in the appropriate relaxation equations. Neglecting CSA, an overall peptide correlation time of 0.69 ns is predicted for *t*-boc-LAWAL-OMe in CD_3OD at 20°C compared with 1.28 ns for *t*-boc-LALALW-OMe. Given these τ_m values and taking into account the effect of measurement error in the T_1 and NOE data, the internal dynamics of the tryptophan residue of *t*-boc-LAWAL-OMe in this isotropic environment are described by a range of τ_e values from 70 to 112 ps and $\mathcal{S}$ values between 0.22 and 0.36. Similarly, for *t*-boc-LALALW-OMe, $68 \leq \tau_e \leq 93$ ps and $0.09 \leq \mathcal{S} \leq 0.17$. The Ch-terminal position of the tryptophan residue in the hexapeptide may account for its lower order parameter. In lysolecithin micelles, the model-free approach applied to *t*-boc-LALALW-OMe predicts a τ_e between 0.87 and 1.08 ns, and an order parameter range of 0.72–0.80, assuming an average τ_m of 14 ns (Saunders, L. 1966. *Biochim. Biophys. Acta.* 125:70) for a typical peptide-micelle complex. In this case, measurement of only two ^{13}C relaxation parameters at a single frequency yields sufficient information, plotted in the form of a composite T_1-NOE solution curve, to constrain the allowed values of the model-free motional parameters within a relatively narrow range. The predicted range of $\mathcal{S}$ and τ_e values for the peptide-micelle complex demonstrate that both the rate and spatial mobility of the indole moiety are markedly restrained in the anisotropic micelle environment relative to free methanol solution. Steady-state fluorescence anisotropy measurements made on the peptides dissolved in methanol or with synthetic lysolecithins in water were used to calculate apparent order parameters for tryptophan motion; these values agree well with order parameters calculated from ^{13}C NMR data. The reported results are relevant to the issue of protein dynamic events occurring on the picosecond time scale predicted by molecular dynamics simulations.

INTRODUCTION

The existence of rapid motions in proteins is now broadly accepted (for reviews, see Careri et al., 1979; Gurd and Rothgeb, 1979), but there is considerable debate regarding the timescales on which such events occur and the amplitudes of the motions. The calculations of Karplus and co-workers (for review, see Karplus and McCammon, 1981) have provided a particularly interesting perspective on protein molecular dynamics. Such simulations have suggested the existence of amino acid sidechain librations

Please address all reprint requests to either Dr. Prendergast or Dr. Kemple.

of considerable magnitude occurring in the low picosecond regime (Ichiye and Karplus, 1983). While such calculations are inherently valuable, the significance of the simulations will be fully realized only when there is experimental verification of the existence, rate, and amplitude of the motions.

In principle, the existence of rapid motions are evident even in x-ray crystallographic data (Petsko and Ringe, 1984), but such data do not readily yield quantitative assessments. In fact, few experimental techniques allow actual quantitation of motional events on this timescale. Fluorescence quenching experiments with oxygen (Lakowicz and Weber, 1973*a*,*b*) and later with other agents (Eftink and Ghiron, 1976) provided early, albeit indirect, evidence for the existence of subnanosecond motions in proteins. Since the quenching agents, especially oxygen, can apparently gain access to fluorophores buried in the protein matrix (devoid of contact with bulk water) during the fluorescence lifetime of the fluorophore, the current assumption is that there are subnanosecond fluctuations of sufficient magnitude allowing such access. Yet again, however, the quenching data do not provide direct evidence of protein dynamics and are subject to an unavoidable uncertainty regarding the precise extent of water accessibility (hence, of dissolved quenching agents) to the fluorophore in the protein matrix (Calhoun et al., 1986).

Measurements of time-resolved anisotropy and of nuclear magnetic resonance (NMR)[1] relaxation parameters have provided some direct experimental data on the rates and amplitudes of subnanosecond motions in proteins. The most unambiguous data have been those derived from measurements of time-dependent anisotropy (Munro et al., 1979; Lakowicz et al., 1983; Eftink, 1983), but those data have generally supported the existence of tryptophan sidechain motions with correlation times >500 ps. Recently, Lakowicz et al., described results of multifrequency phase fluorometry measurements done up to 2 GHz modulation frequency (Lakowicz et al., 1986); the results suggest the existence of a tryptophan indole ring motion with a correlation time of ~25 ps. It is important to note, however, that these measurements were performed on amino acid sidechain motions in peptides, not in proteins. In studies done on lysozyme, analogous measurements have so far failed to show the existence of low picosecond motions (Gratton et al., 1985). Evidence for subnanosecond mobility in proteins has recently been adduced from a reinterpretation of fluorescence lifetime data in terms of fluorescence lifetime distributions. The inference has been made that the distributions arise from the existence of conformational substates which interconvert on a subnanosecond timescale (Gratton et al., 1985; Engh et al., 1986; James and Ware, 1986; Alcala et al., 1987). Again, however, quantitation of the extent and speed of the motions is not yet possible from such data. In principle, ^{13}C NMR relaxation techniques can be used to detect and quantify picosecond motions but are often of limited value due to the low natural abundance of the isotope which necessitates the use of high and frequently unattainable protein concentrations. With selective enrichment the method becomes particularly appealing and measurement of NMR relaxation parameters has clearly demonstrated the occurence of very rapid motions in proteins and peptides (Niu et al., 1979; Eakin et al., 1975; Jones et al., 1976; Blakeley et al., 1978; Deber et al., 1978; Cohen et al., 1979; Harina et al., 1980; Matta et al., 1980; Wooten et al., 1981; Hughes et al., 1984).

For initial experiments with relatively simple systems, both ^{13}C NMR and steady-state fluorescence techniques were applied to study the dynamics of the indole sidechain of tryptophan labeled with ^{13}C in the δ_1 carbon atom with the expectation that the results obtained from both methods would agree. The rationalization of this assumption is as follows. The ^{13}C NMR analysis of motion depends on assessment of the dynamics of the $^{13}C\delta_1$-H vector, while fluorescence anisotropy decay depends on measurement on the reorientation of the emission transition dipole. For indole, both the $^{13}C\delta_1$-H vector and the fluorescence emission dipole lie approximately in the plane of the heterocyclic ring. Thus, the motion assessed from fluorescence data should correlate with motional information derived from ^{13}C NMR observation of the $^{13}C\delta_1$-H vector. The use of oligopeptides allowed examination of cases where the rotational correlation time of both the peptides and the tryptophan sidechain were fast (relative to much larger proteins, for example) and therefore easily accessible to observation by ^{13}C NMR relaxation methods. In particular, we sought to demonstrate the effects of various isotropic and anisotropic solvent environments, namely, organic solvents and aqueous lipid micelles, on both the fluorescence- and NMR-derived orientational order parameter, and on the effective correlation time of the solvent-exposed ^{13}C-labeled tryptophan residue. Results shown below indicate that the differences in order parameter values determined from fluorescence and ^{13}C NMR are quite small.

Two hydrophobic oligopeptides, *t*-boc-LAWAL-OMe[2] and *t*-boc-LALALW-OMe, which consist entirely of aliphatic residues excepting the single tryptophan residues, were synthesized by solid-phase techniques. The amino and carboxy termini were protected by *t*-butyloxycarbonyl

[1] *Abbreviations used in this paper:* NMR, nuclear magnetic resonance; FT, Fourier transform; T_1, spin-lattice relaxation time; T_2, spin-spin relaxation time; NOE, nuclear Overhauser effect; CSA, chemical shift anisotropy; TMS, tetramethylsilane; HPLC, high-pressure liquid chromatography; *t*-boc-, *t*-butyloxycarbonyl-; -OMe, -O-methylester; DPH, 1,6-diphenyl-1,3,5,-hexatriene; NATA, N-acetyltryptophanamide; *t*-BuOH, *t*-butylalcohol; AcOH, acetic acid; DMPC, dimyristoyl-L-α-phosphatidylcholine; DPPC, dipalmitoyl-L-α-phosphatidylcholine; DSPC, distearoyl-L-α-phosphatidylcholine.

[2] Oligopeptides are referred to by standard IUB single letter nomenclature to which protecting group abbreviations are appended.

and methyl ester functions, respectively, to enhance hydrophobicity and thereby facilitate study of these peptides in nonaqueous environments. In order to examine the dynamics of the tryptophan sidechain by ^{13}C NMR, the indole sidechain was >95% enriched with ^{13}C at the $C\delta_1$ position in the ring (Branchini et al., 1987). In designing these experiments, it was assumed (*a*) that the rigidity of the indole ring should mean that the movement of any one atom in the indole moiety (observed by NMR relaxation measurements) faithfully tracks the motion of the entire ring (observed by fluorescence anisotropy); (*b*) that the dipolar interaction between the carbon and its attached proton is the major NMR relaxation mechanism, although chemical shift anisotropy may contribute somewhat; and (*c*) that the near planar, rigid geometry of the indole ring limits its motional freedom to rotations about the two proximal bonds in the sidechain (χ_1 and χ_2 dihedral angles).

Longer aliphatic sidechains with multiple degrees of freedom usually demonstrate considerable motional complexity and correspondingly complex spectral density functions have been invoked to describe the motions. A conceptually simpler, model-free approach was originally applied by Lipari and Szabo (1982*a*,*b*) to a few resolvable sidechain resonances of myoglobin, dihydrofolate reductase, and bovine pancreatic trypsin inhibitor. The approach was also used by Hughes et al. (1984) in the analysis of ^{13}C spin-lattice relaxation times for ribonuclease S′ complexes using selectively ^{13}C-enriched S-peptide. More recently, Henry et al. (1986) have applied the methodology to the analysis of backbone dynamics of detergent-solubilized M13 coat protein. In all cases, specific values were obtained for the effective ^{13}C-H vector correlation time τ_e and for the corresponding generalized order parameter $\mathcal{S}$. However, as Lipari and Szabo have shown (1982*a*,*b*), not only may there be a pronounced effect of experimental error in the predicted values for the model-free motional parameters, but also caution is advised in ascribing validity to $\mathcal{S}$ and τ_e values that fall outside of certain semiempirically determined ranges.

In this paper, spin-lattice relaxation times (T_1 values) and steady-state NOE values measured for the $^{13}C\delta_1$-labeled tryptophan sidechain of two hydrophobic oligopeptides are used to determine the internal dynamics of the indole ring appended to the peptide backbone. Distinctly different behavior of the tryptophan sidechain in two hydrophobic 'solvents', CD_3OD and lysolecithin-D_2O micelles, is reflected in the values of the motional parameters derived from the relaxation data. The effect of error in T_1 and NOE measurements on the derived dynamic information is explicitly assessed. The fluorescence- and NMR-derived order parameter values are also interpreted in terms of likely geometrical constraints on the motion of the indole sidechain. The results show (*a*) good agreement between the values for sidechain order parameter calculated from ^{13}C NMR and fluorescence data; (*b*) that the apparent rotational correlation times of the (presumably spatially unrestrained) tryptophan sidechain in monomeric and oligomeric peptides are on the order of 100 ps in methanol, and an order of magnitude greater in the micellar environment; (*c*) that the spatial restriction of the tryptophan sidechain motion reflected by NMR and fluorescence order parameters is not severe in methanol in spite of probable peptide oligomerization, while the micellar environment imposes considerable motional constraints on sidechain mobility; and (*d*) that although there are clear limitations to current formalisms for calculation of local motions of amino acid sidechains from NMR data, the model-free approach, if carefully applied, does yield quantitatively reasonable correlation times. Finally, the implications of these results for interpretation of recent molecular dynamics simulations are discussed.

MATERIALS AND EXPERIMENTAL PROCEDURES

Synthesis of $^{13}C\delta_1$-L-Tryptophan

The synthetic pathway is outlined in Fig. 1. Proton and ^{13}C NMR spectra (Fig. 2) of the compound clearly indicate incorporation of the label at the appropriate position. Details of the conditions of synthesis are provided by Branchini et al. (1987). The synthesis of the ^{13}C-labeled L-amino acid used in these experiments was carried out by Cambridge Isotope Laboratories, Woburn, MA.

Peptide Synthesis

Di-*t*-butyldicarbonate (Sigma Chemical Co., St. Louis, MO) was used to prepare *t*-boc-$^{13}C\delta_1$-L-tryptophan. Peptides were synthesized using conventional solid-phase methods: *t*-boc-LAWAL-OMe and *t*-boc-LALALW-OMe were prepared on chloromethyl resin and cleaved by transesterification by methanol. The peptides were then purified by HPLC on a semi-preparative C8 reverse-phase column (Brownlee Laboratories, Santa Clara, CA); peptides eluting as single peaks were considered to be homogeneous and were used without further purification. Fast-atom bombardment mass spectroscopy (on a Kratos 500 mass spectrometer; Kratos Analytical Instruments, Ramsey, NJ) was used to verify the molecular weights of the isotopically-labeled synthetic peptides. The HPLC-purified peptides were also examined by thin-layer chromatography on silica gel (60 μm), in *t*-BuOH:AcOH:pyridine:H_2O (5:1:3:4 vol/vol). The *t*-boc protecting group was removed after chromatography by exposing the plates to HCl fumes before ninhydrin treatment. Both purified peptides chromatographed as single spots.

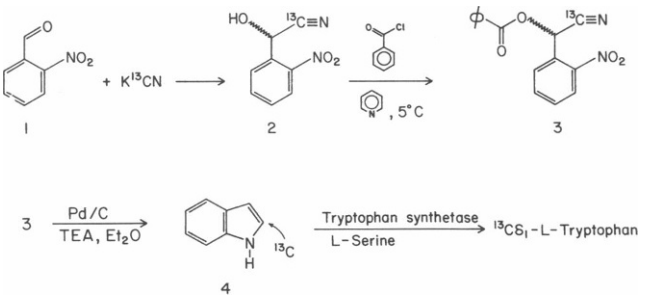

FIGURE 1. Synthetic route to $^{13}C\delta_1$-L-tryptophan.

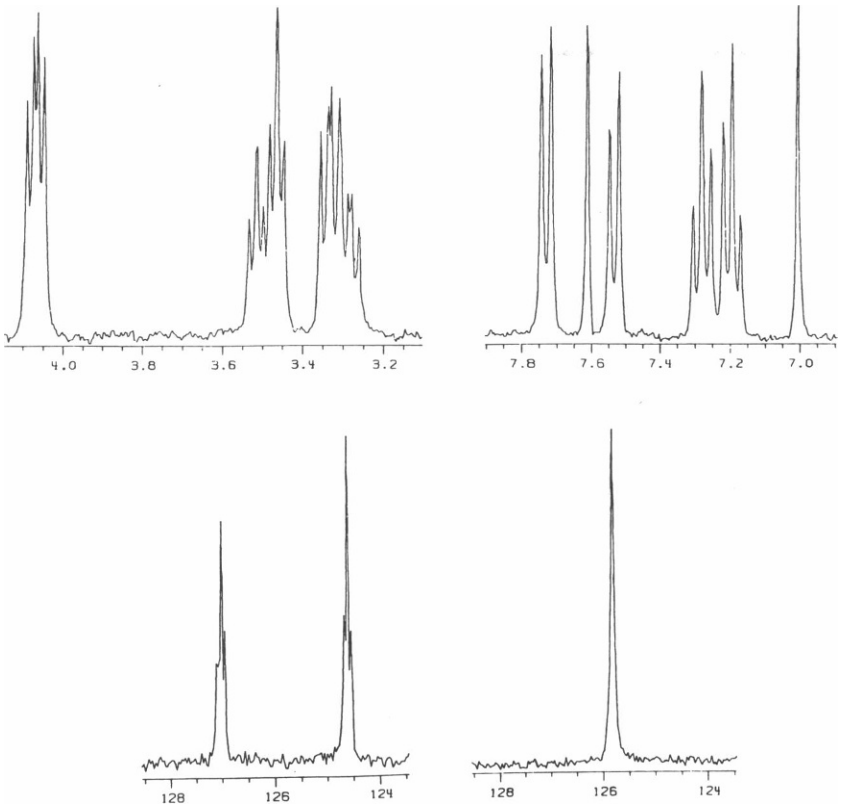

FIGURE 2. 300 MHz ^1H and 75.4 MHz ^{13}C NMR spectra of $^{13}C\delta_1$-L-tryptophan in D_2O, pH 7.0, 20°C. Chemical shift values, given in ppm, are relative to internal TMS.

Preparation of Lysophosphatidylcholine: Peptide Mixed Micelles

For the NMR experiments, peptide (1.98 mM) and lipid (egg lysophosphatidylcholine, 396 mM) were co-dissolved in $CHCl_3$ with the majority of the solvent then removed by rotary evaporation. After removal of residual solvent by overnight vacuum extraction, ~2.5 ml D_2O was added to the sample to obtain a lipid to peptide mole ratio of ~200:1. The mixture was then transferred to a 12-mm NMR tube and vigorously shaken resulting in a slightly turbid solution. For measurements of fluorescence anisotropy, solvent was removed by rotary evaporation from ~1 ml of a dilute (<10 μM) peptide solution in methanol, and a synthetic lysophosphatidylcholine (monomyristoyl-, monopalmitoyl-, or monostearoyl-L-α-phosphatidylcholine) in H_2O was added to obtain approximately a 200:1 lipid to peptide molar ratio.

NMR Spectroscopy

T_1 and steady-state NOE measurements were performed at 75.4 MHz on an NT-300 FT spectrometer (IUPUI) (Nicolet Magnetics Corp., Fremont, CA) and at 50.3 MHz on a Varian XL-200 FT spectrometer (Varian Associates, Inc., Palo Alto, CA) (Purdue University). ^{13}C chemical shifts were measured relative to internal dioxane (67.37 ppm; Shindo et al., 1978) and are reported as ppm downfield from the resonance of TMS. Proton spectra were also acquired at 300 and 200 MHz on the two spectrometers. ^1H chemical shifts were measured relative to an internal TMS reference. Measurements on the 300 MHz spectrometer were made in 12-mm tubes containing peptides in CD_3OD at concentrations of 4.88 mM (*t*-boc-LAWAL-OMe) and 1.89 mM (*t*-boc-LALALW-OMe). Measurements on the 200 MHz instrument were performed on the same samples transferred to 20-mm tubes. Broadband noise decoupling of the protons was used for T_1 and NOE measurements at 75.4 MHz. WALTZ decoupling (Shaka et al., 1983) was used for T_1 and NOE measurements at 50.3 MHz. All T_1 determinations employed a 180°-τ-90° inversion-recovery pulse sequence with a delay of 5 s. Gated decoupling was used to measure the NOE, collecting alternate scans (with and without NOE) into adjacent memory blocks. A delay of 10 s was used between observation pulses in the NOE determinations due to the nonexponential decay of this relaxation parameter. At 75.4 MHz, relaxation data were collected as 8 K points with a spectral width of ±4,000 Hz using quadrature phase detection. At 50.3 MHz, relaxation data were collected as 4 K data points with a spectral width of ±5,300 Hz. Measurements on both peptides were performed at a probe temperature of 20 (±1)°C.

Fluorescence Spectroscopy

Fluorescence spectra were recorded on an MPF-66 fluorometer (Perkin, Elmer, Inc., Norwalk, CT) (λ_{ex} = 280 nm, 2 nm bandpass; λ_{em} = 290–450 nm). Steady-state fluorescence anisotropy measurements on samples with tryptophan-containing peptides in methanol or synthetic lysolecithins were collected on an SLM 4800 fluorometer (SLM Instruments, Inc., Champaign, IL). Measurements were made in the L-format of this instrument. The excitation wavelength was 300 nm (1 nm bandpass). The fluorescence emission was collected through a WG 345 cut-on filter (Schott Glass Technologies Inc., Duryea, PA) to eliminate Rayleigh and Raman scattering artifacts. Measurements were made at 20°C and 40°C. Anisotropy measurements on DPH dissolved in dioxane or mixed with synthetic lysolecithins were also made with the SLM 4800 (λ_{ex} = 360 nm, with a KV 418 cut-on filter in the emission path) at 20°C and 40°C.

DATA ANALYSIS

There are basically two ways currently to estimate motional properties from NMR relaxation data, particularly if they are to be compared with values derived from fluorescence data. One may invoke a relatively simple

formalism if some basic assumptions are satisfied, while more complex systems require a more selective approach.

In both approaches, it is assumed that the principal method of relaxation is via a single magnetic dipole–dipole interaction between the carbon and the attached proton; this is a common assumption which has been shown generally to be valid in other systems (*e.g.*, see London, 1980). Moreover, we assume that the aromatic ring is planar and rigid, and therefore that the motion of the $^{13}C\delta_1$-H vector is at least reasonably representative of the rotation of the entire aromatic moiety. There is ample precedent for this assumption given the similarity in T_1 values for carbon atoms (bearing a single proton) in aromatic rings (*e.g.*, see Alger et al., 1980). Under this assumption, we reasoned that for free tryptophan in a simple solvent it was valid to assume isotropic rotation. Thus, for calculation of the rotational correlation time of free tryptophan a simple formalism was employed.

For dipole–dipole relaxation of a ^{13}C atom having a single bound proton and satisfying the condition of extreme narrowing ($\omega_C \ll 1/\tau_c$, where ω_C is the carbon resonance frequency, and τ_c is the single correlation time)

$$T_1^{-1} = \left(\frac{\hbar^2\gamma_C^2\gamma_H^2}{r_{CH}^6}\right)\tau_c, \tag{1}$$

where T_1^{-1} is the dipolar-spin lattice relaxation rate, $\hbar$ is Planck's constant divided by 2π, γ_C and γ_H are the magnetogyric ratios of ^{13}C and ^1H, respectively, and r_{CH} is the distance between the carbon being considered and its bound proton (1.09 Å), (*cf.* Abragam, 1961).

The situation is less clear cut with structurally more complex peptides and proteins. For such systems we have used an analytic approach based on the compact spectral density equation proposed by Lipari and Szabo (1982*a*)

$$J(\omega) = \frac{2}{5}\left[\frac{\mathcal{S}^2\tau_m}{1+\omega^2\tau_m^2} + \frac{(1-\mathcal{S}^2)\tau}{1+\omega^2\tau^2}\right], \tag{2}$$

where

$$\tau^{-1} = \tau_m^{-1} + \tau_e^{-1}. \tag{3}$$

The spectral density is a function of (*a*) the Larmor frequencies of the ^{13}C nucleus and its bound proton, (*b*) an overall correlation time for the macromolecule τ_m, (*c*) an effective correlation time for the observed internal motion τ_e, and (*d*) a generalized order parameter $\mathcal{S}$, which describes the spatial restriction of the internal motion. Application of Eq. 2 depends on the ability of a single correlation time τ_m to adequately describe the overall motion of the macromolecule. This seems reasonable given the small size of these peptides. However, for larger proteins or peptides this would not necessarily be true because they may possess distinct structural domains, exhibit fast segmental motion, or possess a nonspherical shape incompatible with the use of a single correlation time. Internal motions observed within one structural domain would then have to be analyzed with respect to the correlation time of that domain.

One evaluates the spectral density of Eq. 2 at the appropriate Larmor frequencies ($\omega_H + \omega_C$, $\omega_H - \omega_C$, ω_H, ω_C) treating the motional parameters ($\mathcal{S}$, τ_e, and τ_m) as independent variables. The resulting spectral density values are then applied to relaxation equations (Lipari and Szabo, 1982*a*) to predict the T_1, T_2, and steady-state NOE corresponding to any given set of motional parameters.

$$T_1^{-1} = \frac{\hbar^2\gamma_C^2\gamma_H^2}{4r_{CH}^6}\left[J(\omega_H - \omega_C) + 3J(\omega_C) + 6J(\omega_H + \omega_C)\right] \tag{4}$$

$$T_2^{-1} = \frac{\hbar^2\gamma_C^2\gamma_H^2}{8r_{CH}^6}\left[4J(0) + J(\omega_H - \omega_C) + 3J(\omega_C) + 6J(\omega_H) + 6J(\omega_H + \omega_C)\right] \tag{5}$$

$$\mathrm{NOE} = 1 + \frac{\gamma_H}{\gamma_C}\left[\frac{6J(\omega_H + \omega_C) - J(\omega_H - \omega_C)}{J(\omega_H - \omega_C) + 3J(\omega_C) + 6J(\omega_C + \omega_H)}\right]. \tag{6}$$

To optimally utilize these relations for analysis of the relaxation data obtained for the oligopeptides, a computer program, NMRFIT, was developed which finds allowed values for the model-free motional parameters $\mathcal{S}$, τ_e, and τ_m given any number of experimental relaxation values at one or more frequencies.[3]

Essentially, reduction of the data amounts to a least-squares fit of the experimentally observed relaxation values to the nonlinear relaxation equations given above (Eqs. 4–6). For example, if only two relaxation values (often T_1 and NOE at a single frequency) are known, the algorithm systematically evaluates the spectral density equation over all values for τ_m specified as physically reasonable; $\mathcal{S}$ and τ_e are adjusted at each τ_m value until the predicted pair of relaxation values matches the experimentally observed values. The results of such calculations may be depicted as solution curves which demonstrate the relationships between $\mathcal{S}$, τ_e, and τ_m for the system. In favorable cases, such as the peptide-micelle system that we investigated, the constraints placed on the values of $\mathcal{S}$ and τ_e define these internal motional parameters with considerable precision. If three or more relaxation values are specified, the algorithm finds a unique solution to the system of relaxation equations (i.e., specific values for $\mathcal{S}$, τ_e, and τ_m), which represents a least-squares fit of the calculated to the observed relaxation values. We show below, however, that the typical expected errors in relaxation measurements advise against the assignment of unique values to the motional parameters; indeed, a range of values for the sidechain correlation time and the generalized order

[3]A compiled version of this program, written for IBM-compatible personal computers, is available from one of the authors (A.J.W.) upon request.

parameter may better describe the actual dynamics of the system.

RESULTS

Graphical Analysis of ^{13}C NMR Relaxation Data

Data from T_1 measurements made on ^{13}C-enriched tryptophan in free D_2O solution were used to calculate its apparent rotational correlation time from Eq. 1. At 20°C, a T_1 value of 1.09 s was observed, from which a τ_c value of 40 ps is predicted. This result agrees well with a 30 ps correlation time determined from fluorescence lifetime-resolved anisotropy data (Lakowicz et al., 1983) for NATA. We (Prendergast, unpublished data) and others (Gratton and Jameson, 1985) have used multifrequency phase/modulation fluorometry to measure the time-dependent anisotropy of free NATA in H_2O. These experiments yielded a rotational correlation time of ~50 ps, which, considering the timescale, is in good agreement with the NMR and fluorescence results just described.

The proton spectra of both peptides (data not shown) confirm their amino acid composition and show the characteristic splitting pattern due to the $^{13}C\delta_1$ label in the tryptophan sidechain. The proton-decoupled 50.3 and 75.4 MHz ^{13}C NMR spectra of *t*-boc-LAWAL-OMe and *t*-boc-LALALW-OMe in CD_3OD at 20°C consist of a single peak centered at 124.4 and 124.6 ppm, respectively, relative to TMS. The coupled spectra show the expected splitting by the single bound porton (^1J = 181.3 Hz).

The integrity of the tryptophan sidechain is readily evaluated by the appearance of the ^{13}C NMR spectrum of these peptides. Degradation of the indole ring usually results from oxidation of the Cγ-Cδ_1 double bond to form a Cδ_1-oxo group, followed by cleavage of the pyrrole ring between Cγ and Cδ_1. The resulting in situ formylkynurenine residue may be further degraded with loss of the Cδ_1 atom (Fontana and Toniolo, 1976). Such events would result in loss of the split ^1H resonance, and ^{13}C chemical shift changes should certainly accompany oxidation at the Cδ_1 atom. Since no such features were ever observed, we conclude that the ^{13}C-labeled indole ring remained intact during the synthesis of the peptides.

T_1 and NOE values were measured for the tryptophan sidechain $^{13}C\delta_1$ atom of both oligopeptides at 50.3 and 75.4 MHz in CD_3OD at 20°C, and at 75.4 MHz for *t*-boc-LALALW-OMe in lysolecithin-D_2O micelles (Table I). A graphical representation of the method used to generate solution curves from single-frequency T_1 and NOE data is depicted in Fig. 3. Each point on the curve corresponds to the intersection of a T_1 and an NOE curve generated for a specific fixed value of the overall peptide correlation time τ_m. A simple T_1 or NOE curve describes all of the possible (allowed) $\mathcal{S}$ and τ_e values consistent with a single value of τ_m and the measured T_1 or NOE value. A composite T_1-NOE solution curve is thus derived from

TABLE I
OBSERVED T_1 AND STEADY-STATE NOE VALUES* AT 50.3 AND 75.4 MHz FOR *t*-boc-LAWAL-OMe IN CD_3OD AND *t*-BOC-LALALW-OMe IN CD_3OD OR LYSOLECITHIN-D_2O AT 20°C

	50.3 MHz		75.4 MHz	
	T_1 *ms*	NOE	*ms*	NOE
t-boc-LALALW-OMe CD_3OD	530	2.80	462	2.65
t-boc-LALALW-OMe CD_3OD	671	2.93	592	2.90
lysolecithin			195	1.54

*Typical errors for T_1 determinations were ± 0.010 s. NOE values are accurate to within ± 5% of the observed value.

multiple intersections of simple T_1 and NOE curves through the range of physically reasonable τ_m values. It should be noted that both types of curves represent exact fits of the model-free $\mathcal{S}$, τ_e, and τ_m motional parameters to an experimentally observed relaxation value or values. The information content of the composite T_1-NOE curve, however, is greater in that an entire range of τ_m values is visually accessible in a single plot. As shown below, this feature can be used to advantage in constraining the values for $\mathcal{S}$ and τ_e by specifying an appropriately narrow (or not so narrow) range of overall correlation times for the macromolecule.

Fig. 3 depicts the construction of a composite T_1-NOE solution curve from three intersections of simple T_1 and NOE curves corresponding to three different τ_m values. The composite T_1-NOE solution curve passes through these intersections as well as all intersections of T_1 and NOE curves that could be constructed (but are not shown) for intermediate τ_m values. The intersecting simple curves of Fig. 3 are related to those shown in a recent study by Henry et al. (1986) on the backbone dynamics of detergent-solubilized M13 coat protein, where plots of $\mathcal{S}^2$ versus $-\log \tau_e$ are generated for eight discrete τ_m values. The intersection (or near intersection) of three or more simple T_1, T_2, or NOE curves is merely a graphical representation of a successful (or nearly so) nonlinear least-squares fit of

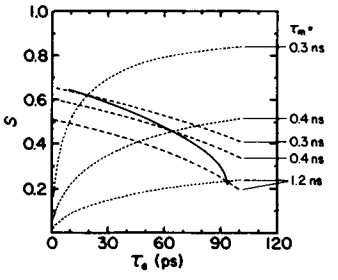

FIGURE 3. Construction of a composite T_1-NOE solution curve for *t*-boc-LAWAL-OMe from intersections of T_1 (———) with NOE (. . . . .) curves generated at three discrete τ_m values (0.3, 0.4, and 1.2 ns). Intermediate points on the T_1-NOE curve correspond to intermediate τ_m values. The solution curves presented in this work graphically depict the constraints placed on the internal dynamics of the tryptophan sidechain (specified in terms of $\mathcal{S}$ and τ_e), which are consistent with any given pair of relaxation values measured at a single spectrometer frequency.

the experimental relaxation data to the model-free motional parameters contained in Eqs. 4–6. No useful information is available from any one of these single relaxation value curves; only the existence of a common intersection (or lack thereof) is meaningful. By contrast, the composite solution curve approach presented here allows one to see, in a single plot, all of the physically allowable values for the motional parameters pertinent to the internal motion of interest (namely, the orientational order parameter $\mathcal{S}$ and the effective correlation time τ_e for the internal motion) given any pair of experimental NMR relaxation values for the same system. As shown below, even an approximate knowledge of the overall correlation time for the macromolecule (estimates of which are easily accessible by other spectroscopic or hydrodynamic measurements) often allows quite narrow constraints to be placed on the allowed values for the internal motional parameters directly from the composite plot.

At each frequency, the internal motion is readily evaluated by plotting $\mathcal{S}$ as a function of τ_e, that is, describing the spatial restriction of the internal motion as a function of its rate. In Fig. 4, computer-generated composite T_1-NOE solution curves show allowed values for $\mathcal{S}$ and τ_e corresponding to the observed T_1 and NOE values for *t*-boc-LAWAL-OMe and *t*-boc-LALALW-OMe in CD_3OD, at both 75.4 and 50.3 MHz. In these plots, the overall peptide correlation time τ_m is varied between ~0.1 and 1.5 ns. In Fig. 5, the same three-dimensional data (actually a single curve in three-space) are plotted as the correlation time for the internal motion τ_e, and generalized order parameter $\mathcal{S}$ versus τ_m. Fig. 6 *a* shows $\mathcal{S}$ versus τ_e for *t*-boc-LALALW-OMe in lysolecithin-D_2O micelles, where τ_m is varied from 0.9 to 200 ns. In all of the $\mathcal{S}$ versus τ_e plots, low τ_m values correspond to the leftmost region of the curves. Interestingly, the functional form of the single-frequency composite T_1-NOE solution curves (Figs. 4 and 5) for the peptides in CD_3OD differs markedly from the curve obtained for *t*-boc-LALALW-OMe in lysolecithin-D_2O (Fig. 6). However, a meaningful interpretation, of these results relies on accurate assessment of the effect that experimental error in the relaxation data may have on the derived model-free motional parameters. In Figs. 4–6, the dashed lines above and below the solid curves demonstrate the effect of concomitant measurement errors in both T_1 and NOE. The upper curves are generated for $T_1 = 0.95 \cdot T_{1obs}$ and for $NOE = 1.05 \cdot NOE_{obs}$, while the lower curves depict $T_1 = 1.05 \cdot T_{1obs}$ and $NOE = 0.95 \cdot NOE_{obs}$. These curves represent the maximal effect (i.e., with respect to deviations in $\mathcal{S}$ and τ_e) of concomitant 5% errors in T_1 and NOE measurements, which are the errors calculated from the experimental data (see Table I).

Inasmusch as the composite solution curves represent a continuum of τ_m values, by specifying a particular τ_m, one can find the corresponding values of $\mathcal{S}$ and τ_e and thus gain immediate information about the internal dynamics of the system assuming one has chosen the appropriate value for the overall correlation time of the molecule. Taking into consideration the effect of measurement error on the derived motional parameters, we find a tryptophan sidechain correlation time of <100 ps, and corresponding $\mathcal{S}$ values between 0.1 and 0.8 for both peptides in CD_3OD at 20°C. These $\mathcal{S}$ and τ_e values obtain for overall peptide correlation times between ~0.1 and 1.5 ns, which for the most part are well above the expected τ_m values for these

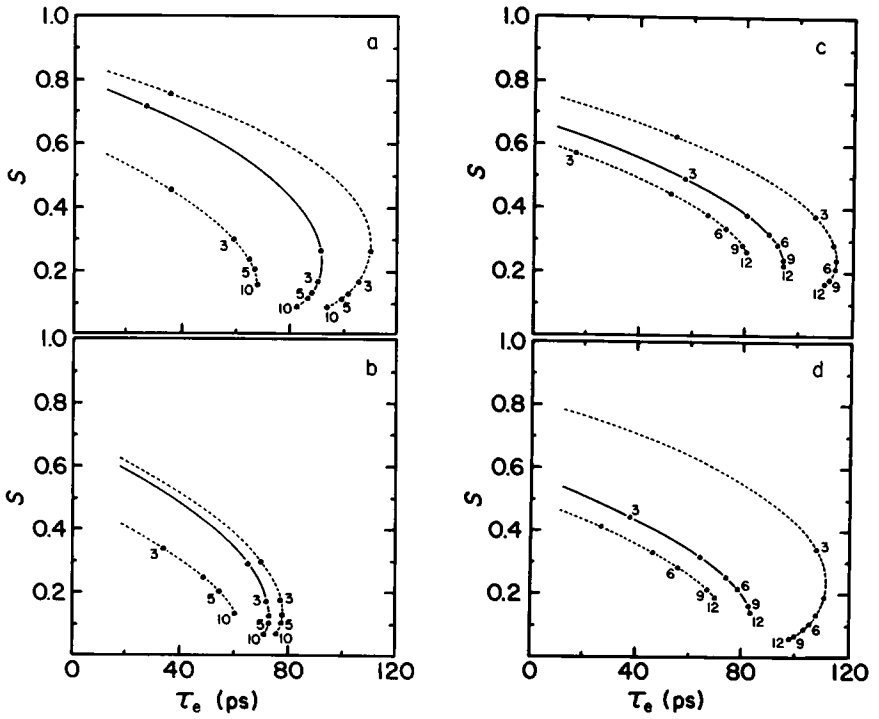

FIGURE 4. Internal dynamics of the tryptophan sidechain of *t*-boc-LALALW-OMe and *t*-boc-LAWAL-OMe in CD_3OD at 20°C calculated for overall peptide correlation times (τ_m values) between ~0.1 and 1.5 ns. (*a*) t-boc-LALALW-OMe, 75.4 MHz; (*b*) *t*-boc-LALALW-OMe, 50.3 MHz; (*c*) *t*-boc-LAWAL-OMe, 75.4 MHz; (*d*) *t*-boc-LAWAL-OMe, 50.3 MHz. Dashed curves represent composite ±5% error limits applied to the experimental relaxation data. Discretely plotted points give τ_e and $\mathcal{S}$ values corresponding to τ_m values of peptide oligomers of aggregation number *n*, where *n* is the number of monomers in an aggregated complex. τ_m values were calculated as described in the text. For *t*-boc-LALALW-OMe, discrete *n* values of (1,2), 3,4,5, and 10 are indicated alongside the appropriate point; for *t*-boc-LAWAL-OMe, τ_m values corresponding to *n* values of (2,3),4,5,6,9, and 12 are plotted.

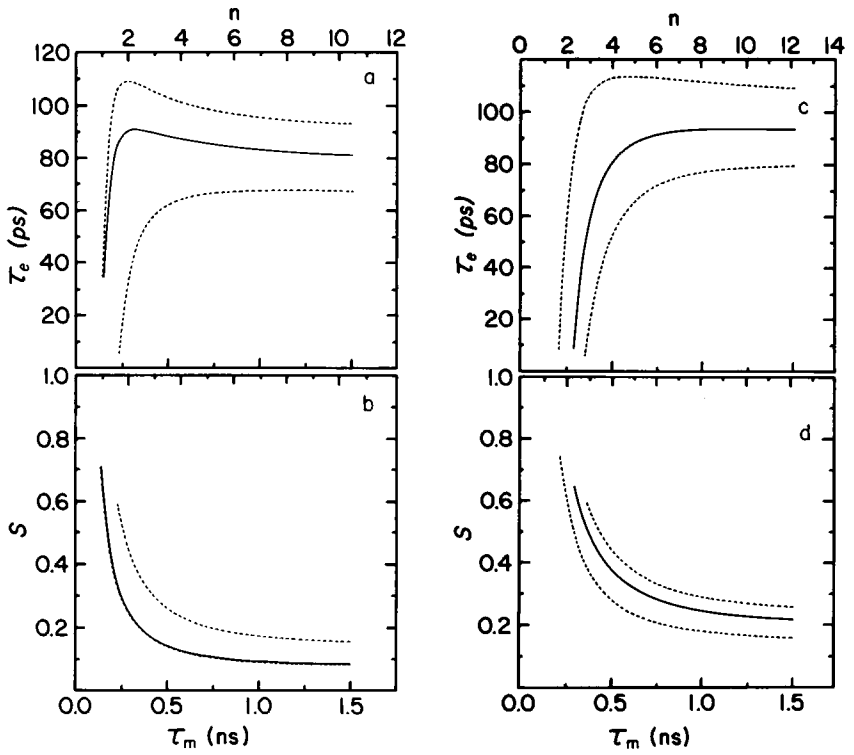

FIGURE 5. Tryptophan sidechain correlation time τ_e, and sidechain order parameter $\mathcal{S}$ plotted as a function of the overall peptide correlation time (τ_m) for *t*-boc-LALALW-OMe (*a,b*) and for *t*-boc-LAWAL-OMe (*c,d*) at 75.4 MHz in CD_3OD at 20°C. Overall peptide correlation times (τ_m values) corresponding to discrete peptide oligomers (*n*) are indicated on the upper abscissa. Dashed curves represent composite ±5% error limits. Similar curves describe results obtained at 50.3 MHz.

small peptides. The Stokes-Einstein relation ($\tau_m = (M/N)\eta\bar{V}/kT$, where M is the molecular weight of the peptide, $N = 6.02 \cdot 10^{23}$, $\eta = 0.597$ cP, $\bar{V} = 0.73$ cm^3 g^{-1}, $k = 1.38 \cdot 10^{-16}$ erg K^{-1}, and $T = 293$ K) predicts a τ_m of 123 and 143 ps, for monomeric *t*-boc-LAWAL-OMe and *t*-boc-LALALW-OMe, respectively, at 20°C in methanol. At the far left end of the solution curves of Figs. 4 and 5, the $\mathcal{S}$ values are quite large (>0.7) and the predicted τ_e values are ≤20 ps. Such values would be sharply inconsistent with the least-squares analysis of the NMR relaxation data and with the fluorescence results obtained for these peptides (see below).

At slightly higher concentrations or at lower temperatures than were used in the NMR experiments, the

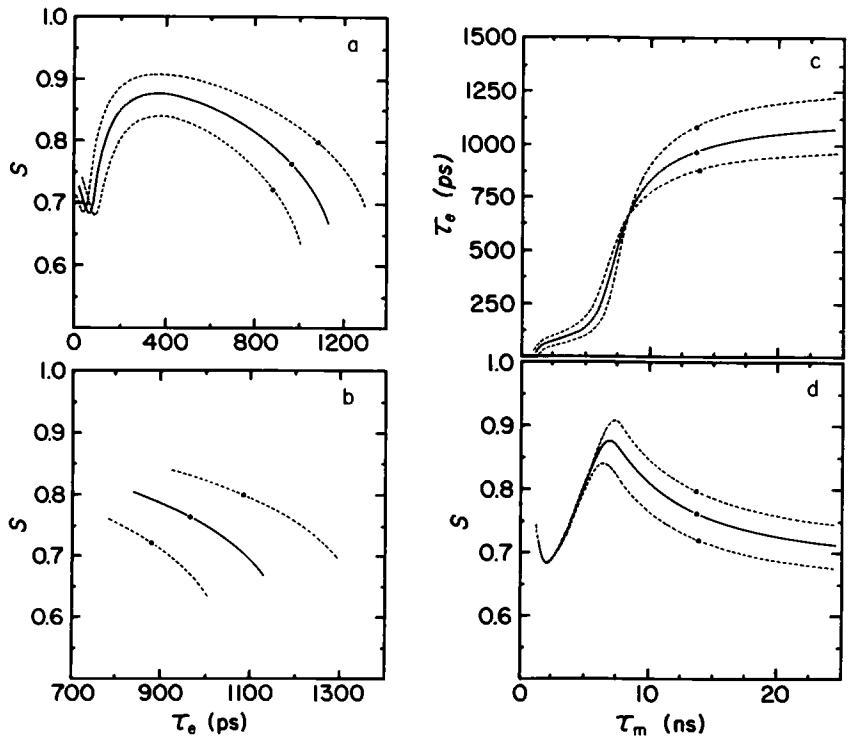

FIGURE 6. Internal dynamics of the tryptophan sidechain of *t*-boc-LALALW-OMe in lysophophatidylcholine-D_2O micelles at 20°C. Data were obtained at 75.4 MHz and calculations were made for τ_m values between 0.9 and 200 ns (*a*); and for τ_m values between 10 and 200 ns (*b*). The tryptophan sidechain correlation time τ_e, and sidechain order parameter $\mathcal{S}$ are shown as a function of the overall peptide correlation time τ_m in (*c,d*). Dashed curves represent ±5% error limits. The single discrete point plotted on each of the solution curves corresponds to the estimated correlation time of 14 ns (Saunders, 1966), for a typical lysophosphatidylcholine micelle.

peptides readily formed needle-shaped crystals from methanol. Larger values for τ_m caused by aggregation of the peptides are therefore quite likely. Thus, in order to assess the extent to which peptide oligomerization is occurring, discrete points are plotted on the $\mathcal{S}$ versus τ_e curves in Figs. 4 and 6 corresponding to τ_m values, based on the Stokes-Einstein relation referred to above, for peptide oligomers of aggregation number n, such that $\tau_{m,\text{oligomer}} = n\tau_{m,\text{monomer}}$. Note that in all of the plots, changes in $\mathcal{S}$ and τ_e become less pronounced with each integer increment in the peptide aggregation number n. The close spacing of the points in Fig. 4 for peptide aggregates containing ~5 or more monomers is illustrative. We show below, in discussing the results of nonlinear least-squares analysis employing three or more ^{13}C NMR relaxation values, that higher order oligomers ($n \geq 5$) of both peptides are probably the predominant species existing in methanol under the conditions of the NMR measurements.

For *t*-boc-LALALW-OMe in lysolecithin-D_2O micelles, the situation is different in that only very loose constraints on τ_m need be specified in order to gain a good first approximation to the values of $\mathcal{S}$ and τ_e in this system. The form of the solution curve allows one to set relatively narrow bounds on the range of values for the internal motional parameters. In Fig. 6 *a*, the overall correlation time τ_m is varied from ~0.9 to 200 ns. Assuming an average Stokes radius of 28 Å for lysophosphatidylcholine micelles (Saunders, 1966), an average correlation time for a spherical micelle would be ~14 ns. Given this value for the τ_m of the peptide embedded in the lipid micelle (as indicated in Fig. 6), $\tau_e = 0.96$ ns with a 5% error range of 0.87-1.08 ns, and $\mathcal{S} = 0.77$ (0.72–0.80). Now, assuming some asymmetry of the micellar particles and no unique value for τ_m, a reasonable lower limit might be ~10 ns. In Fig. 6 *b*, $\mathcal{S}$ versus τ_e is replotted with a minimum τ_m of 10 ns. Thus, for τ_m between 10 and 200 ns, $0.84 \leq \tau_e \leq 1.10$ ns, and $0.67 \leq \mathcal{S} \leq 0.81$ (no measurement errors are included here). Fig. 6 *a* also shows that setting a lower bound on τ_m is not necessary to impose these limits on allowed values for $\mathcal{S}$. Thus, in this favorable case, measurement of only two relaxation values at a single frequency for a sidechain atom apparently allows the desired information about its motion to be derived even if a very large range of τ_m values is assumed.

Least-Squares Analysis of ^{13}C NMR Relaxation Data

The analysis of the relaxation data can be extended to simultaneously solve by a nonlinear least-squares fitting procedure, a system of three or more relaxation equations. Given the three model-free motional parameters ($\mathcal{S}$, τ_e, and τ_m), specific solutions for the system of equations (Eqs. 4–6) require at least three experimental relaxation values as input. Graphically, a unique solution should ideally appear as a common intersection of three (or more) simple T_1, T_2, or NOE curves generated at the correct value for τ_m. Henry et al. (1986) show such an intersection for one alanine methyl group, yet point out that more typically one finds a triangle comprising three intersections of two curves. In contrast, we find that it should almost always be possible to find a unique solution to the system of equations given three relaxation values as input, if the experimental relaxation values are not outside of theoretical limits imposed by the equations themselves (e.g., with no CSA for a carbon bearing a single proton, $1.153 \leq \text{NOE} \leq 2.988$). Given four or more relaxation values, however, a least-squares fit will rarely, if ever, give a χ^2 of zero. Least-squares predicted values for the model-free motional parameters for both oligopeptides in CD_3OD are compiled in Table II. Least-squares analysis was performed for each of four possible combinations of three relaxation values in addition to using all four of the relaxation values (i.e., T_1 and NOE values measured at two frequencies). This approach was taken so that an aberrant relaxation value might become more readily apparent by giving results inconsistent with least-squares results obtained in its absence. No large discrepancies, however, were noted,

TABLE II
COMBINED LEAST-SQUARES ANALYSIS OF OLIGOPEPTIDE ^{13}C RELAXATION DATA OBTAINED AT TWO SPECTROMETER FREQUENCIES WITH AND WITHOUT A CONTRIBUTION FROM CHEMICAL SHIFT ANISOTROPY*

50.3 MHz		75.4 MHz	τ_m ns	τ_e ps	$\mathcal{S}$	χ^2
t-boc-LAWAL-OMe, CD_3OD, 20°C						
T_1 NOE		T_1	1.62	94.7	0.133	0.008
	+ CSA		1.44	89.9	0.075	0.002
T_1 NOE		NOE	0.37	39.0	0.438	~0
	+ CSA		0.81	86.8	0.113	~0
T_1		T_1 NOE	1.18	84.9	0.213	0.012
	+ CSA		1.17	90.3	0.089	0.002
NOE		T_1 NOE	0.37	56.9	0.491	~0
	+ CSA		0.91	96.3	0.106	~0
T_1 NOE		T_1 NOE	0.69	84.7	0.258	0.013
	+ CSA		1.19	90.1	0.089	0.002
t-boc-LALALW-OMe, CD_3OD, 20°C						
T_1 NOE		T_1	1.63	77.9	0.043	0.006
	+ CSA		0.60	76.6	0.000	0.003
T_1 NOE		NOE	0.54	72.7	0.134	~0
	+ CSA		0.57	74.2	0.000	0.012
T_1		T_1 NOE	1.19	78.5	0.062	0.007
	+ CSA		0.60	76.5	0.000	0.012
NOE		T_1 NOE	0.59	87.6	0.126	~0
	+ CSA		0.71	77.5	0.000	0.012
T_1 NOE		T_1 NOE	1.28	77.8	0.067	0.007
	+ CSA		0.60	76.4	0.000	0.013

*A chemical shift anisotropy $\Delta\delta$ of 180 ppm was used for those calculations which included this relaxation term (Eqs. 7–9). When $\mathcal{S} \simeq 0$, the spectral density at a given frequency depends only upon $\tau^{-1} = \tau_e^{-1} + \tau_m^{-1} \simeq \tau_e^{-1}$.

which increases the confidence in the values for the model-free motional parameters derived using all of the available data.

Graphically, exact ($\chi^2 \simeq 0$) fits are exemplified in Fig. 7, where three relaxation values yield a common intersection when curves are plotted at the appropriate τ_m value. When all four relaxation values are simultaneously fitted, the parallelogram of Fig. 8 results, comprising four intersections of two curves. This nonunique result, when compared with the other exact fits, attests to the problems associated with exact fitting obtained with three relaxation equations in three unknowns ($\mathcal{S}$, τ_e, and τ_m), especially the problem of over-interpreting the unique values that result. The degree of nonideality of the least-squares fit using T_1 and NOE data at both observations frequencies is reflected in the χ^2 values given in Table II.

While measurement error in the relaxation values most likely makes the greatest contribution to the χ^2, inadequacies of the model contribute as well. The smaller values of

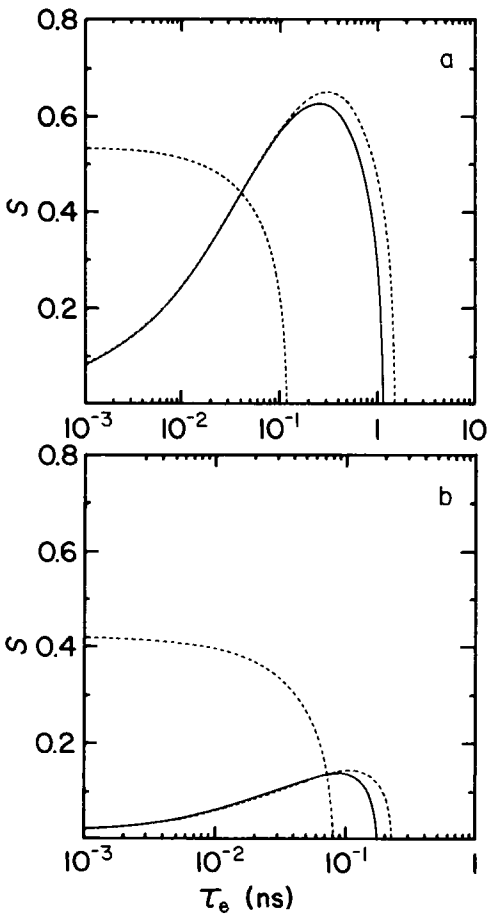

FIGURE 7. Graphical representation of nonlinear least-squares analyses of NMR data demonstrating exact fits obtained with three relaxation values measured at two frequencies. T_1 and NOE curves generated from 50.3 MHz data (.....) and an NOE curve generated from 75.4 MHz data (———) intersect at a common point given an overall peptide correlation time (τ_m) of 0.37 ns for *t*-boc-LAWAL-OMe (*a*), or with τ_m = 0.54 ns for *t*-boc-LALALW-OMe (*b*).

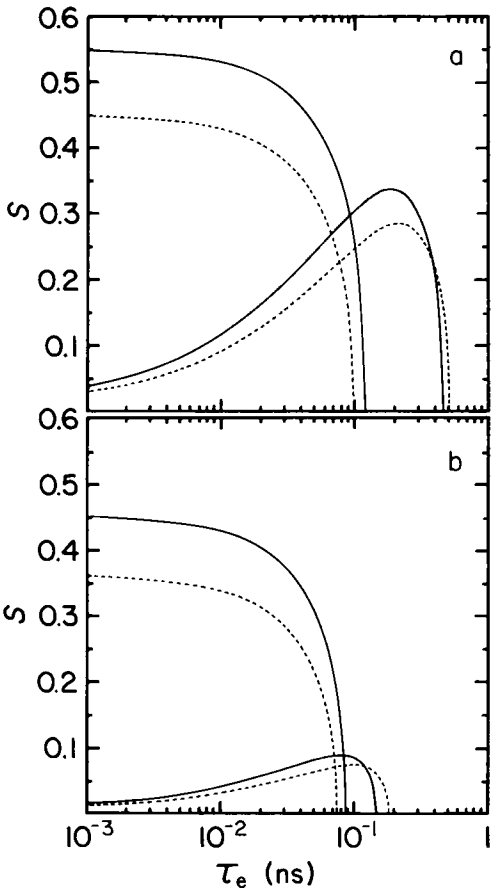

FIGURE 8. Graphical representation of the result of simultaneous nonlinear least-squares fitting of the model free parameters $\mathcal{S}$, τ_e, and τ_m to experimental T_1 and NOE relaxation values measured at both 50.3 (.....) and 75.4 MHz (———) in CD_3OD at 20°C. For *t*-boc-LAWAL-OMe, the least-squares fit overall peptide correlation time (τ_m) is 0.69 ns (*a*); for *t*-boc-LALALW-OMe, τ_m = 1.28 ns (*b*).

T_1 at the higher frequency (Table I) indicate immediately that CSA must contribute to the relaxation. Assuming an axially symmetric chemical shift tensor $\underline{\delta}$, those contributions are (Lipari and Szabo, 1982*a*; Noggle and Schirmer, 1971)

$$T_{1CSA}^{-1} = (\Delta\delta)^2\omega_C^2 J(\omega_C) \tag{7}$$

$$T_{2CSA}^{-1} = (1/6)(\Delta\delta)^2\omega_C^2[4J(0) + 3J(\omega_C)], \tag{8}$$

while the NOE equation becomes

$$\text{NOE} = 1 + \frac{(\gamma_H/\gamma_C)[6J(\omega_H+\omega_C) - J(\omega_H-\omega_C)]}{J(\omega_H-\omega_C) + 3J(\omega_C) + 6J(\omega_C+\omega_H)} + [4r_{CH}^6(\Delta\delta)^2\omega_C^2/\gamma_C^2\gamma_H^2]\, J(\omega_C), \tag{9}$$

where $\Delta\delta = \delta_\parallel - \delta_\perp$. We have explicitly included the contribution of CSA to spin-lattice relaxation in the NOE expression. To our knowledge, a $\Delta\delta$ value has not been measured for the $C\delta_1$ atom in L-tryptophan. Here, a $\Delta\delta$ value of 180 ppm was used for all of the least-squares determinations that included CSA; this value is typical for

carbonyl or aromatic carbon atoms (Pines et al., 1972). The results as modified by CSA are included in Table II.

Least-squares analysis of the relaxation data shows some interesting patterns for both peptides. Without CSA, when two T_1 values and a single NOE are used in the analysis, lower order parameter values are generally predicted compared with analyses employing two NOE's and a single T_1 value. When all relaxation values are fitted simultaneously, one obtains an intermediate result. With the inclusion of CSA in the analysis, the $\mathcal{S}$ values are smaller and the motional parameters predicted using various combinations of T_1 and NOE data converge. The smaller $\mathcal{S}$ values are in large part due to the effect of CSA on the NOE. In particular, for *t*-boc-LALALW-OMe the fits gave $\mathcal{S} \simeq 0$. In this instance, the experimental NOE values exceeded the maximum NOE allowed by Eq. 8 with $\Delta\delta = 180$ ppm, indicating that the actual $\Delta\delta$ is likely to be smaller in this peptide. The significant perturbation of the least-squares fit values with addition of CSA and the internal consistency of those results (at least for *t*-boc-LAWAL-OMe) point out that CSA should certainly be included in analysis of high field relaxation data. Comparison of the $\mathcal{S}$ and τ_e values predicted for the two peptides in CD_3OD suggests that tryptophan sidechain motion is somewhat slower and more restricted in the pentapeptide. This result is consistent with its central position in the amino acid sequence of *t*-boc-LAWAL-OMe, while the C-terminal location of the indole sidechain in the hexapeptide would likely favor greater mobility.

Values for $\mathcal{S}$, τ_e, and τ_m in Table II resulting from least-squares analyses correspond to the rightmost region of the $\mathcal{S}$ versus τ_e curves of Figs. 4 and 5, which strongly suggests that the oligopeptides are aggregated in methanol solution under the conditions of the NMR measurements. In the absence of CSA, least-squares fits to all of the relaxation data obtained at both 75.4 and 50.3 MHz predicted tryptophan sidechain $\mathcal{S}$ and τ_e values of 0.26 and 85 ps, with an overall peptide correlation time (τ_m) of 0.69 ns for *t*-boc-LAWAL-OMe in CD_3OD at 20°C; and $\mathcal{S} = 0.07$, $\tau_e = 78$ ps, with a τ_m of 1.28 ns for *t*-boc-LALALW-OMe under the same conditions. A τ_m value of 0.69 ns for the *t*-boc-LAWAL-OMe oligomer corresponds to a time- and ensemble-averaged aggregation number $\langle \bar{n} \rangle = 5.6$ peptide monomers, while for *t*-boc-LALALW-OMe, a τ_m value of 1.28 ns gives $\langle \bar{n} \rangle = 9.0$. However, as the brackets and superscripted bar notation for n implies, these values do not necessarily indicate that discrete peptide oligomers containing ~6 and 9 monomers, respectively, exist in methanol solution. Indeed, the monomer constituents of a given oligomer are probably in fast exchange with the free peptide on the NMR timescale since heterogeneity is not observed for any of the resonances of the ^1H NMR spectra of both oligopeptides in methanol solution. As noted above, given the close spacing of the n values along the rightmost region of the $\mathcal{S}$ versus τ_e curves, a rather narrow range of $\mathcal{S}$ and τ_e values corresponds to a wide range of overall correlation time values; hence, no precise quantitation of the extent of peptide oligomerization is possible, except to acknowledge the existence of higher order aggregates ($n \geq 5$) for both hydrophobic oligopeptides.

It is worth noting that one can use the composite T_1-NOE solution curves of Figs. 4 and 5 to specify a relatively narrow range of $\mathcal{S}$ and τ_e values falling within composite 5% error limits for the relaxation values (dashed curves). Thus, for *t*-boc-LAWAL-OMe in CD_3OD at 20°C, the internal dynamics of the tryptophan residue (in the absence of CSA) are described by a range of values $70 \leq \tau_e \leq 112$ ps and $0.22 \leq \mathcal{S} \leq 0.36$, at an overall peptide correlation time τ_m 0.69 ns ($\langle \bar{n} \rangle = 5.6$). Similarly, for *t*-boc-LALALW-OMe, $68 \leq \tau_e \leq 93$ ps, $0.09 \leq \mathcal{S} \leq 0.17$ at $\tau_m = 1.28$ ns ($\langle \bar{n} \rangle = 9.0$). The existence of rather small $\mathcal{S}$ and τ_e values suggests that the tryptophan sidechain is relatively unrestrained for these peptides in methanol solution, its correlation time being slower than that of free tryptophan only by a factor of ~2. Apparently, peptide aggregation has little effect on the dynamics accessible to the tryptophan sidechain, which is intuitively contradictory. However, the observation is not without precedent; the single-tryptophan peptide melittin, for example, experiences very little change in its dynamic properties as detected by fluorescence anisotropy techniques upon aggregation of the monomer to form a well-characterized tetrameric particle (Lakowicz et al., 1985).

Steady-State Fluorescence Spectra and Anisotropy Data

Since fluorescence anisotropy data can provide information on the extent to which a fluorophore is restricted in its motion (Kinosita et al., 1977; Engel and Prendergast, 1981; Jähnig, 1979), such measurements were made to corroborate the NMR data. The fluorescence emission spectra of the peptides in micelles (data not shown) indicate moderately restricted solvent accessibility ($\lambda_{max} = 341$ nm) relative to free tryptophan in water, consistent with partitioning of the peptides with the micelles. Similar values of λ_{max} were observed for the oligopeptides in anhydrous methanol, which is typical for tryptophan-containing peptides (Jain et al., 1985). While these data are not sufficient to prove that there was residual peptide in the aqueous phase, this is unlikely given the distinct insolubility of both peptides in aqueous media and the fact that the emission spectra were not further altered by higher lipid to peptide ratios.

Estimations of the order parameter of the tryptophan sidechain motion in the micelles from measurements of fluorescence steady-state anisotropy values rely currently on assumption of a model in which an axially symmetric fluorophore is rotating isotropically within a conical potential (Kinosita, 1979; Jähnig, 1979; Engel and Prendergast, 1981). As Hare (1983) has discussed, for fluorophores in

hindered environments, steady-state anisotropy values are likely to be close in value to the limiting hindered anisotropy r_∞, whereupon the order parameter can be calculated from the relation $S^2 = \bar{r}/r_o$, $\bar{r}$ being the measured steady-state anisotropy and $\bar{r}_o$ the maximum anisotropy at the excitation wavelength employed. The most accurate assessment of S, however, comes from the relation $r/r_o = ([1-S^2]/[1 + \tau_f/\tau]) + S^2$ (e.g., see Lakowicz et al., 1985) where τ_f is the fluorescence lifetime with all other parameters retaining their aforementioned meanings. This relation implies that for oligomers in lipid complexes of the peptides, where τ (given by Eq. 3) is small relative to τ_f, the estimate of S from steady-state fluorescence anisotropy is likely to be good. If, however, τ is not much smaller than τ_f, then the order parameter calculated as $(\bar{r}/\bar{r}_o)^{1/2}$ will be overestimated relative to its actual value. Since fluorescence lifetimes were not measured for these oligopeptides, all S values were calculated as $(\bar{r}/\bar{r}_o)^{1/2}$. Thus, for monomeric or oligomeric peptides in free solution, the calculated order parameter values are certainly overestimated, which must be borne in mind when interpreting these values.

The results of fluorescence anisotropy measurements on the peptides in methanol and in micelles of synthetic lysophospholipids are given in Table III. For the oligopeptides in methanol, the fluorescence- and NMR-derived order parameter values are comparable. A variety of synthetic lysophospholipids were used in the fluorescence anisotropy experiments in order to assess the effect of increasing acyl chain length on the derived order parameter values and to facilitate comparision with DPH in the same micellar environments. As expected, S values increase with chain length for DPH, which can reasonably be assumed to be embedded amidst the hydrocarbons of the micellar structure. However, the similar values for tryptophan sidechain and DPH anisotropy do not necessarily mean that the peptide indole moiety and DPH are similarly disposed in the micelle environment. Nevertheless, tryptophan sidechain order parameter values derived from fluorescence anisotropy data are interpreted here in terms of motion in a conical potential (Kinosita et al., 1977) through a maximal cone semi-angle of θ_c (Table III), which decreases with acyl chain lenght from 58° to 52° for *t*-boc-LALALW-OMe, and from 56° to 53° for *t*-boc-LAWAL-OMe. The NMR-derived range of $\mathcal{S}$ values in egg phosphatidylcholine at 20°C (0.72–0.80) are somewhat larger and correspond to $31° \leq \theta_c \leq 37°$. Notably, no physically reasonable τ_m value for the micelle-peptide complex (1–200 ns) would allow NMR-derived $\mathcal{S}$ values lower than ~0.7 ($\theta_c \leq 38°$); (see Fig. 6 *d*).

TABLE III
STEADY-STATE FLUORESCENCE ANISOTROPY VALUES, DERIVED ORDER PARAMETERS, AND CONE SEMI-ANGLES FOR *t*-BOC-LAWAL-OMe, *t*-BOC-LALALW-OMe, AND DPH IN METHANOL OR DIOXANE AND SYNTHETIC LYSOLECITHINS*

	$\bar{r}$		$S(\theta_c)$	
	20°C	40°C	20°C	40°C
t-boc-LAWAL-OMe				
methanol	0.006	0.005	0.14 (77°)	0.13 (78°)
MMPC	0.075	0.057	0.49 (52°)	0.43 (56°)
MPPC	0.092	0.063	0.55 (49°)	0.45 (55°)
MSPC	0.099	0.071	0.57 (47°)	0.48 (53°)
t-boc-LALALW-OMe				
methanol	0.008	0.005	0.16 (75°)	0.13 (78°)
MMPC	0.083	0.053	0.51 (51°)	0.41 (58°)
MPPC	0.091	0.064	0.54 (49°)	0.45 (55°)
MSPC	0.101	0.074	0.57 (47°)	0.49 (52°)
1,6-diphenyl-1,3,5-hexatriene				
dioxane	0.007	0.006	0.13 (78°)	0.12 (78°)
MMPC	0.113	0.082	0.54 (49°)	0.46 (54°)
MPPC	0.136	0.095	0.59 (46°)	0.49 (52°)
MSPC	0.181	0.107	0.68 (40°)	0.52 (51°)

*Order parameter values were calculated using $r_0 = 0.315$, for tryptophan-containing peptides (Lakowicz et al., 1985), and $r_0 = 0.39$ for DPH (Lakowicz et al., 1979). Measurement errors for $\bar{r}$ determinations are ± 0.003.

Although egg lysophosphatidylcholine, which contains a variety of acyl chain lengths as well as unsaturated species, was used in the NMR experiments, the dynamic character of the micellar structure would argue against a dramatically different environment for the peptide in egg phosphatidylcholine compared with homogeneous synthetic lysophospholipids. Nonetheless, an increased content of unsaturated lipids would presumably have the effect of disordering the lipid hydrocarbon environment, thereby decreasing the NMR-derived tryptophan sidechain order parameter values relative to values observed in the saturated synthetic lysophospholipid micelles. As noted above, the fluorescence anisotropy data, however, predict order parameter values that are somewhat smaller than those derived from ^{13}C NMR relaxation data; thus, an alternative explanation is necessary. It is possible that this is a concentration-dependent effect since the NMR experiments required more than 100-fold higher lipid concentrations in order to achieve a 200:1 lipid to peptide ratio.

The calculated values for the motional parameters found for the *t*-boc-LALALW-OMe micelle preparation should also be interpreted with regard to possible perturbation of micelle structure by the peptide. The number of lipid molecules in a typical spherical micelle prepared from lysolecithin has been calaculated to be 181 (Saunders, 1966). Thus, for a 200:1 ratio of lipid to peptide, it may be assumed that <1 peptide molecule would be incorporated per micelle if the peptide is uniformly distributed. This small number aruges against perturbation of the micellar structure by peptide–peptide interactions. Nonetheless, repeated attempts to form stable liposomes at 20°C with either egg phosphatidylcholine or DMPC in the presence

of a small amount of peptide (200:1 lipid to peptide, [mol/mol]) were unsuccessful. It remains possible, however, that peptide oligomers also form in the micelle environment, which may perturb the lipid structure to a greater extent than would a monomeric peptide. Notably, Jacobs and White (1986) have recently shown with differential scanning calorimetry that a tryptophan-containing tripeptide (AWA-O-*t*-butyl) may cause considerable membrane perturbation. Our experience with *t*-boc-LAL-ALW-OMe would seem to corroborate their observations.

DISCUSSION

Efforts to characterize peptide motions in solution by ^{13}C NMR relaxation measurements are complicated by the high concentrations of peptide necessitated by the relative insensitivity of the ^{13}C nucleus. Selective labeling ameliorates the problem, yet does not guarantee that peptide–peptide interactions will not occur. Measurements of ^{13}C relaxation times in peptide solutions have often implicated peptide aggregation as being responsible for unexpectedly short T_1 values (Howarth and Lilley, 1978). Even at the relatively low peptide concentrations that were used in the NMR studies (<5 mM), the propensity of these peptides to crystallize from methanol at either slightly higher concentrations or at lower temperatures was remarkable. Given this observation, peptide aggregation is almost certainly occurring in the NMR experiments, as evidenced by predicted τ_m values larger than expected for the monomeric oligopeptides in methanol. Obviously, studies of temperature-dependent changes in dynamics would be quite informative in these systems. The fluorescence studies, on the other hand, were done at concentrations nearly 100-fold less. The low order parameter values predicted by NMR and fluorescence data for the oligopeptides in methanol solution suggests that peptide aggregation does not significantly affect the motional character of the tryptophan sidechain in these systems. This apparent aggregation satisfied one of our objectives, namely, to show that tryptophan sidechain motion is detectable in the context of a larger macromolecular assembly by the methods described. The relevance of this result to the study of protein dynamics is clear. It should also be noted that the formation of stable peptide aggregates may not be occurring in the NMR experiments; quasi-stable transient aggregates may have the effect of slowing the observed overall correlation time of the peptides (at higher peptide concentrations) yet still allow tryptophan sidechain motion comparable with the monodisperse state.

The correlation times suggested by out NMR results are generally an order of magnitude greater than those derived from in vacuo molecular dynamics simulations (Karplus and McCammon, 1981; Ichiye and Karplus, 1983). While the effects of solvent friction on accessible residues will likely lengthen correlation times (Doster, 1983), molecular dynamics simulations including solvent have not explicitly demonstrated this (Ghosh and McCammon, 1987). The correlation time measured by NMR relaxation for free tryptophan (40 ps) was comparable with that found for tryptophan motion in the oligopeptides (68–112 ps), indicating the existence of rapid motion for the solvent-exposed tryptophan sidechain in these small peptides. However, at this point, little can be said about the motions of sidechains buried in the interior of proteins. For such residues, the amplitude of motion will be restricted by protein packing constraints and the librational motions could be in the low picosecond regime.

The experiments with the peptides in the lipid micelle suggest that the correlation time for tryptophan sidechain motion in this system is slowed by a factor of ~10 relative to its value in methanol solution, assuming that the overall correlation time of the peptide matches that estimated for the micelle. The order parameter for this motion, however, is predicted to be high ($\mathcal{S} > 0.6$), regardless of the overall correlation time (Fig. 6). While the precise spatial disposition of the sidechain cannot be determined from the data, the significant motional restriction suggests considerable interaction with the fatty acyl sidechains of the micellar phospholipids. The shifts in the fluorescence emission spectra support this notion, but are not pronounced enough for us to infer that the indole ring is entirely protected from the aqueous environment. Given the order parameters calculated from the NMR and the fluorescence data, the tryptophan sidechain appears to be markedly constrained in this system. Although constraint per se is not a determinant of rate of rotational motion, the fact that the motions are constrained suggests that there are strong interactions between the fluorophore and the lipid such that the motion of the fluorophore and lipid appear to be in concert.

Overall, the data we have presented on the ^{13}C-enriched tryptophan and the results of the application of the Lipari and Szabo method for the analysis of relaxation data confirm the usefulness of ^{13}C NMR spectroscopy for the measurement of molecular motions. The good consonance of the fluorescence and NMR determined order parameters is also reassuring. However, it is clear that more complex systems will need to be examined, especially ones which lend themselves well to molecular dynamics calculations. We are currently studying the dynamics of melittin and melittin analogues labeled with ^{13}C in the peptide backbone (^{13}C-α-glycine) and sidechain ($^{13}C\delta_1$-L-tryptophan). Melittin forms a tetramer of MW = 11,400 in solutions of high salt concentration, and the x-ray crystal structure of this form is known (Terwilliger and Eisenberg, 1982), thus allowing studies of internal sidechain dynamics on a protein-like system.

We wish to thank the Purdue Univeristy Biochemical Magnetic Resonance Laboratory at West Lafayette, Indiana, and the Physics Department of Indiana University-Purdue University at Indianapolis (IUPUI) for use of their NMR facilities. Particular thanks go to S. R. Wassall,

B. D. Nageswara Rao, and B. D. Ray for helpful comments and suggestions throughout the work and during preparation of the manuscript. The figures in this paper were kindly prepared by P. Callahan.

This work was supported by NI486K0521 from the Office of Naval Research, by National Institutes of Health GM34847, and by a grant from the Minnesota Affiliate of the American Heart Association. The NTC-300 NMR spectrometer at IUPUI was purchased with partial support from National Science Foundation PCM 8018725. Purdue Univeristy Biochemical Magnetic Resonance Laboratory is supported by National Institutes of Health RR01077. K^{13}CN used in the synthesis of ^{13}C-tryptophan was provided in part by the Los Alamos Stable Isotope Resource which is supported by National Institutes of Health RR02231 and the United States Department of Energy/Office of Health and Environmental Research Stable Isotope Program.

This manuscript is taken in part from a thesis of Arthur J. Weaver in partial fulfillment of the requirements for the Ph.D. degree.

Received for publication 12 October 1987 and in final form 5 February 1988.

REFERENCES

Abragam, A. 1961. The Principles of Nuclear Magnetism. Ch. VIII. Oxford University Press, London.

Alcala, R., E. Gratton, and F. G. Prendergast. 1987. Interpretation of Flourescence Decays in Proteins Using Continuous Lifetime Distributions. *Biophys. J.* 51:925–936.

Alger, T. D., W. D. Hamill, Jr., R. K. Pugmire, D. M. Grant, G. D. Silcox, and M. Solum. 1980. Carbon-13 Spin-Lattice Relaxation in Condensed Aromatic Compounds. *J. Phys. Chem.* 84:632–636.

Blakeley, R. L., L. Cocco, R. E. London, T. E. Walker, and N. A. Matwiyoff. 1978. Nuclear Magnetic Resonance Studies on Bacterial Dihydrofolate Reductase Containing [Methyl-^{13}C] Methionine. *Biochemistry.* 17:2284–2293.

Branchini, B. R., F. G. Prendergast, G. A. Spencer, J. D. Hagdahl, B. D. Ray, and M. D. Kemple. 1987. Synthesis of Racemic [2'-^{13}C] Tryptophan. *J. Labeled Comp. & Radiopharm.* 24:637–643.

Calhoun, D. B., J. M. Vanderkooi, G. R. Holtom, and S. W. Englander. 1986. Protein Fluorescence Quenching by Small Molecules: protein penetration versus solvent exposure. *Proteins:* 1:109–115.

Careri, G., P. Fasella, and E. Gratton. 1979. Enzyme Dynamics: the statistical physics approach. *Annu. Rev. Biophys. Bioeng.* 8:69–97.

Cohen, J. S., J. Yariv, A. J. Kalb, L. Jacobson, and Y. Shechter. 1979. ^{13}C-NMR Analysis of Methionine Sulfoxide in Protein. *J. Biochem. Biophys. Methods.* 1:145–151.

Deber, C. M., M. A. Moscarello, and D. D. Wood. 1978. Conformational studies on ^{13}C-enriched human and bovine myelin basic protein, in solution and incorporated into liposomes. *Biochemistry.* 17:898–903.

Doster, W. 1983. Viscosity scaling and protein dynamics. *Biophys. Chem.* 17:97–103.

Eakin, R. T., L. O. Morgan, and N. A. Matwiyoff. 1975. Carbon-13 nuclear magnetic resonance spectroscopy of [2'-^{13}C] carboxymethylcytochrome C. *Biochemistry.* 14:4538–4543.

Eftink, M. R., and C. A. Ghiron. 1976. Exposure of tryptophanyl residues in proteins. Quantitative determination by fluorescence quenching studies. *Biochemistry.* 15:672–680.

Eftink, M. R. and C. A. Ghiron. 1977. Exposure of tryptophanyl residues and protein dynamics. *Biochemistry.* 16:5546–5551.

Eftink, M. R. 1983. Quenching-resolved emission anisotropy studies with single and multitryptophan-containing proteins. *Biophys. J.* 43:323–334.

Engel, L. W. and F. G. Prendergast. Values for and significance of order parameters and "cone angles" of fluorophore rotation in lipid bilayers. *Biochemistry.* 20:7338–7345.

Engh, R. A., L. X.-Q. Chen, and G. R. Fleming. 1986. Conformational dynamics of tryptophan-a proposal for the origin of the non-exponential fluorescence decay. *Chem. Phys. Lett.* 126:365–372.

Fontana, A., and C. Toniolo. 1976. The chemistry of tryptophan in peptides and proteins. *Prog. Chem. Organ. Natural Products.* 33:309–449.

Ghosh, I., and J. A. McCammon. 1987. Side-chain rotational isomerization in proteins. *Biophys. J.* 51:637–641.

Gratton, E., and D. M. Jameson 1986. New approach to phase and modulation resolved spectra. *Anal. Chem.* 57:1694–1697.

Gurd, F. R. N., and T. M. Rothgeb. 1979. Motions in proteins. *Adv. Protein Chem.* 33, 73–165.

Hare, F. 1983. Simplified derivation of angular order and dynamics of rod-like fluorophores in models and membranes. *Biophys. J.* 42:205–218.

Harina, B. M., D. F. Dyckes, M. R. Willcott, and W. C. Jones. 1980. Denaturation studies by ^{13}C nuclear magnetic resonance on modified basic pancreatic trypsin inhibitor using the novel S-[^{13}C]-methylmethionyl probe. *J. Am. Chem. Soc.* 102:1120–1124.

Henry, G. D., J. H. Weiner, and B. D. Sykes. 1986. Backbone dynamics of a model membrane protein: ^{13}C NMR spectroscopy of alanine methyl groups in detergent-solubilized M13 coat protein. *Biochemistry.* 25:590–598.

Hochstrasser, R. M., and D. K. Negus. 1984. Picosecond Fluorescence Decay of Tryptophans in Myoglobin. *Proc. Natl. Acad. Sci. USA.* 81:4399–4403.

Howarth, O. W., and D. M. Lilley. 1978. Carbon-13 NMR of peptides and proteins. *Prog. NMR Spectroscopy.* 12:1–40.

Hughes, L. T., J. S. Cohen, A. Szabo, C. Niu, and S. Matsuura. 1984. ^{13}C NMR studies of the molecular dynamics of selectively ^{13}C-enriched ribonuclease complexes. *Biochemistry.* 23:4390–4394.

Ichiye, T., and M. Karplus. 1983. Fluorescence depolarization of tryptophan residues in proteins: a molecular dynamics study. *Biochemistry.* 22:2884–2893.

Jacobs, R. E., and S. H. White. 1986. Mixtures of a series of homologous hydrophobic peptides with lipid bilayers: a simple model system for examining the protein-lipid interface. *Biochemistry.* 25:2605–2612.

Jähnig, F. 1979. Structural order of lipids and proteins in membranes; evaluation of fluorescence anisotropy data. *Proc. Natl. Acad. Sci. USA.* 76:6361–6365.

Jain, M. K., J. Rogers, L. Simpson, and L. M. Gierasch. 1985. Effect of tryptophan derivatives on the phase properties of bilayers. *Biochim. Biophys. Acta.* 816:153–162.

James, D. R., and W. R. Ware. 1986. Recovery of underlying distributions of lifetimes from fluorescence decay data. *Chem. Phys. Lett.* 126:7–11.

Jones, W. C., T. M. Rothgeb, and F. R. N. Gurd. 1976. Nuclear magnetic resonance studies of sperm whale myoglobin specifically enriched with ^{13}C in the methionine methyl groups. *J. Biol. Chem.* 251:7452–7460.

Karplus, M., and J. A. McCammon. 1981. The internal dynamics of globular proteins. *CRC Crit. Rev. Biochem.* 9:293–349.

Kinosita, K., Jr., S. Kawato, and A. Ikegami. 1977. A theory of fluorescence polarization decay in membranes. *Biophys. J.* 20:289–305.

Lakowicz, J. R., and G. Weber. 1973*a*. Quenching of fluorescence by oxygen. A probe for structural fluctuations in macromolecules. *Biochemistry.* 12:4161–4170.

Lakowicz, J. R., and G. Weber. 1973*b*. Quenching of protein fluorescence by oxygen. Detection of structural fluctuations in proteins on the nanosecond time scale. *Biochemistry.* 12:4171–4179.

Lakowicz, J. R., F. G. Prendergast, and D. Hogen. 1979. Differential polarized phase fluorometric investigations of diphenylhexatriene in lipid bilayers. Quantitation of hindered depolarizing rotations. *Biochemistry.* 18:508–519.

Lakowicz, J. R., and G. Weber. 1980. Nanosecond segmental mobilities of tryptophan residues in protein observed by lifetime-resolved fluorescence anisotropies. *Biophys. J.* 32:591–601.

Lakowicz, J. R., B. P. Maliwal, H. Cherek, and A. Balter. 1983. Rotational freedom of trytophan residues in proteins and peptides. *Biochemistry.* 22:1741–1752.

Lakowicz, J. R., G. Laczko, I. Grycznyski, and H. Cherek. 1985. Measurement of subnanosecond anisotropy decays of protein fluorescence using frequency-domain fluorometry. *J. Biol. Chem.* 261:2240–2245.

Lakowicz, J. R., G. Laczko, and I. Gryczynski. 1986. 2-GHz frequency-domain fluorometry. *Rev. Sci. Instrum.* 57:2499–2506.

Levy, R. M., and A. Szabo. 1982. Initial fluorescence depolarization of tyrosines in proteins. *J. Am. Chem. Soc.* 104:2073.

Lipari, G., and A. Szabo. 1982*a*. Model-free approach to the interpretation of nuclear magnetic resonance relaxation in macromolecules. I. Theory and range of validity. *J. Am. Chem. Soc.* 104:4546–4559.

Lipari, G., and A. Szabo. 1982*b*. Model-free approach to the interpretation of nuclear magnetic resonance relaxation in macromolecules. II. Analysis of experimental results. *J. Am. Chem. Soc.* 104:4559–4570.

London, R. E. 1980. Magnetic Resonance in Biology. Vol 1. J. S. Cohen, editor. John Wiley and Sons, New York.

London, R. E., and J. Avitabile. 1978. Calculated ^{13}C NMR relaxation parameters for a restricted internal diffusion model. Application to methionine relaxation in dihydrofolate reductase. *J. Am. Chem. Soc.* 100:7159–7165.

Matta, M. S., M. E. Landis, T. B. Patrick, P. A. Henderson, M. W. Russo, and R. L. Thomas. 1980. ^{13}C-enriched S-methyl probe at the active site of an enzyme: [S-{^{13}C} methylmethionine-192]-α-chymotrypsin. *J. Am. Chem. Soc.* 102:7151–7152.

Munro, I., I. Pecht, and L. Stryer. 1979. Subnanosecond motions of tryptophan residues in proteins. *Proc. Natl. Acad. Sci. USA.* 76:56–60.

Niu, C. -H., S. Matsuura, H. Shindo, and J. S. Cohen. 1979. Specific peptide-protein interactions in the ribonuclease S′ system studied by ^{13}C-enriched peptides. *J. Biol. Chem.* 254:3788–3796.

Noggle, J. H., and R. E. Schirmer. 1971. The Nuclear Overhauser Effect: Chemical Applications. Academic Press Inc. New York.

Nordlund, T., and D. A. Podolski. 1983. Streak camera measurement of tryptophan and rhodamine motions with picosecond time resolution. *Photochem. Photobiol.* 38:665–669.

Petsko, G. A., and D. Ringe. 1984. Fluctuations in protein structure from x-ray diffraction. *Ann. Rev. Biophys. Bioeng.* 13:331–371.

Pines, A., M. G. Gibby, and J. S. Waugh. 1972. Protein-enhanced nuclear induction spectroscopy: ^{13}C chemical shielding anistropy in some organic solids. *Chem. Phys. Lett.* 15:373–376.

Saunders, L. 1966. Molecular aggregation in aqueous dispersions of phosphatidyl and lysophosphatidyl cholines. *Biochim. Biophys. Acta.* 125:70–74.

Shaka, A. J., T. Frenkiel and R. Freeman. 1983. NMR broad-band decoupling with low radiofrequency power. *J. Magn. Reson.* 52:159–163.

Shindo, H., W. Egan, and J. S. Cohen. 1978. Studies of individual carboxyl groups in proteins by carbon-13 nuclear magnetic resonance spectroscopy. *J. Biol. Chem.* 253:6751–6755.

Terwilliger, T. C., and D. Eisenberg. 1982. The structure of melittin. II. Interpretation of the structure. *J. Biol. Chem.* 257:6016–6022.

Wooten, J. B., J. S. Cohen, and A. Schejter. 1981. pH-Induced conformational transitions of ferricytochrome C: a carbon-13 and deuterium nuclear magnetic resonance study. *Biochemistry.* 20:5394–5402.